

# Interacting dark sectors in light of DESI DR2

Rahul Shah,<sup>1,\*</sup> Purba Mukherjee,<sup>2,†</sup> and Supratik Pal<sup>1,‡</sup>

<sup>1</sup>*Physics and Applied Mathematics Unit, Indian Statistical Institute,  
203, B.T. Road, Kolkata 700 108, India*

<sup>2</sup>*Centre for Theoretical Physics, Jamia Millia Islamia,  
New Delhi 110025, India*

Possible interaction between dark energy and dark matter has previously shown promise in alleviating the clustering tension, without exacerbating the Hubble tension, when BAO data from SDSS DR16 is combined with CMB and SNIa datasets. With the recent DESI BAO DR2, there is now a compelling need to re-evaluate this scenario. We combine DESI DR2 with Planck 2018 and Pantheon+ SNIa datasets to constrain interacting dark matter dark energy models, accounting for interaction effects in both the background and perturbation sectors. Our results exhibit similar trends to those observed with SDSS, albeit with improved precision, reinforcing the consistency between the two BAO datasets. In addition to offering a resolution to the  $S_8$  tension, in the phantom-limit, the dark energy equation of state exhibits an early-phantom behaviour, aligning with DESI DR2 findings, before transitioning to  $w \sim -1$  at lower redshifts, regardless of the DE parametrization. However, the statistical significance of excluding  $w = -1$  is reduced compared to their non-interacting counterparts.

Cosmology today is an observationally driven field that has made tremendous progress in recent years, thanks to expansive and novel data from cutting-edge instruments and observatories. In particular, the Dark Energy Spectroscopic Instrument (DESI)<sup>1</sup> has reignited excitement by hinting at a dynamically evolving dark energy (DE) equation of state (EoS), which challenges the standard cosmological constant ( $\Lambda$ ) paradigm [1]. This has led to a surge of studies investigating DESI's apparent non- $\Lambda$  preference [2–18], with the recent data release 2 (DR2) [19] continuing this trend.

On top of the excitement surrounding evolving dark energy, DESI DR2 also provides the most precise and up-to-date baryon acoustic oscillations (BAO) dataset [19]. This warrants a re-evaluation of key previous results, especially those based on the SDSS BAO data, by the authors of the present paper [20]. The tensions afflicting the  $\Lambda$ CDM model are now well-known, with the Hubble tension and clustering tension inspiring hundreds of studies on alternative physical models, experimental systematics, and novel analysis pipelines [21–23]. Among these, interactions in the dark sector, i.e., between dark matter and dark energy, have been extensively explored in the literature (see [24] and references therein). Certain interaction setups have shown promise in alleviating specific cosmological tensions (see [20, 25–30] and references therein).

We consider the interacting dark matter dark energy (iDMDE) setup outlined in Sec. 2 of [20], which is compatible with dynamical dark energy (DDE) scenarios. This makes it well-suited for re-examination in light of DESI DR2, given the mild preference for an EoS devi-

ating from  $w = -1$ . Here, we replace the SDSS DR16 BAO data used in [20] with DESI DR2. We constrain the models using a combination of Planck 2018 TTTEEE + low- $\ell$  + low-E + lensing data [31–33], DESI DR2 BAO distance measurements (as listed in Table IV of [19]), and Pantheon+ SNIa compilation [34]. We employ a modified version of CLASS [35, 36] (derived from [37, 38]) and MontePython [39, 40], with the DESI DR2 likelihood internally developed and cross-checked for consistency with results obtained from the DESI DR2 likelihood in Cobaya [41].

Furthermore, when considering perturbations in both dark sectors to investigate the impact of evolving DE on clustering, it is well-known that the perturbation equations contain a term (the “doom factor” [42]) in the denominator that diverges at the phantom line ( $w = -1$ ) [43]. To extract meaningful information, it is therefore customary to perform the analysis separately for the phantom and non-phantom regions (as described in [20, 29]). In the non-interacting case, this crossing is handled smoothly using the parametrized post-Friedmann (PPF) formalism [44] (as also done by the DESI collaboration). However, in interacting models, the energy exchange between dark matter and dark energy introduces additional terms in the perturbation equations. To avoid degenerate effects from combining PPF with the interaction term, we divide the parameter space into non-phantom  $w(z) > -1$  and phantom  $w(z) < -1$  regimes. This also allows for distinct prior ranges on the DE EoS parameter,  $w_0$ , while preserving the exact perturbation equations. Additionally, we fix the sound speed of dark energy perturbations to  $c_s^2 = 1$ .

Given the  $S_8$  values reported in [45–47], the results from SDSS BAO [20] indicate that a phantom EoS helps alleviate the  $S_8$  tension without worsening the  $H_0$  tension. Whereas, a non-phantom EoS tends to exacerbate the  $S_8$  tension, and slightly worsen the  $H_0$  tension. We find similar conclusions with DESI DR2 regarding the

\* [rahul.shah.13.97@gmail.com](mailto:rahul.shah.13.97@gmail.com) (corresponding author)

† [purba16@gmail.com](mailto:purba16@gmail.com)

‡ [supratik@isical.ac.in](mailto:supratik@isical.ac.in)

<sup>1</sup> <https://www.desi.lbl.gov/>

Parameters	CPL	i-CPL	JBP	i-JBP
$\Omega_b h^2$	$0.02244 \pm 0.00014$	$0.02246 \pm 0.00013$	$0.02250 \pm 0.00014$	$0.02253 \pm 0.00013$
$\Omega_c h^2$	$0.11905 \pm 0.00087$	$0.1558^{+0.0087}_{-0.0071}$	$0.1184 \pm 0.0012$	$0.151^{+0.012}_{-0.0097}$
$100\theta_s$	$1.04199 \pm 0.00029$	$1.04202 \pm 0.00028$	$1.04204 \pm 0.00029$	$1.04210 \pm 0.00027$
$\ln(10^{10} A_s)$	$3.045 \pm 0.014$	$3.048 \pm 0.015$	$3.051 \pm 0.016$	$3.053 \pm 0.016$
$n_s$	$0.9677 \pm 0.0034$	$0.9684 \pm 0.0036$	$0.9695 \pm 0.0039$	$0.9702 \pm 0.0035$
$\tau$	$0.0558 \pm 0.0071$	$0.0570^{+0.0071}_{-0.0080}$	$0.0585 \pm 0.0080$	$0.0601^{+0.0081}_{-0.0091}$
$Q$	-	$0.390^{+0.10}_{-0.084}$	-	$0.34^{+0.13}_{-0.11}$
$w_0$	$-0.837 \pm 0.056$	$> -1.04$	$-0.807 \pm 0.085$	$> -1.06$
$w_a$	$-0.59^{+0.23}_{-0.21}$	$-0.33 \pm 0.15$	$-1.09 \pm 0.53$	$-0.33 \pm 0.30$
$H_0$	$67.57 \pm 0.59$	$67.92 \pm 0.52$	$67.57 \pm 0.70$	$68.07 \pm 0.53$
$\Omega_{m0}$	$0.3114 \pm 0.0057$	$0.388^{+0.021}_{-0.018}$	$0.3102 \pm 0.0072$	$0.376^{+0.027}_{-0.023}$
$\sigma_{8,0}$	$0.8098 \pm 0.0090$	$0.661^{+0.024}_{-0.031}$	$0.806 \pm 0.011$	$0.673^{+0.034}_{-0.044}$
$S_8$	$0.8250 \pm 0.0098$	$0.751^{+0.014}_{-0.015}$	$0.819 \pm 0.012$	$0.751^{+0.018}_{-0.021}$
$\chi^2_{min}$	4199	4201	4202	4204
$-\ln \mathcal{L}_{min}$	2099.70	2100.32	2100.84	2102.04

TABLE I: The mean and  $1\sigma$  constraints obtained for interacting (phantom regime) and non-interacting models considered in the present work, using combined Planck 2018 + DESI DR2 BAO + Pantheon+ datasets.

status of  $H_0 - S_8$  tensions. Because of the previous success of the phantom regime and its continued validity with the latest datasets, we focus on phantom results in the main paper. For the non-phantom setup, we refer the reader to Appendix A, where we outline its key characteristics.

As representative DDE models, we consider two widely accepted parametrizations of the DE EoS: the Chevallier-Polarski-Linder (CPL) [ $w(a) = w_0 + w_a(1 - a)$ ] [48, 49] and the Jassal-Bagla-Padmanabhan (JBP) [ $w(a) = w_0 + w_a a(1 - a)$ ] [50]. Table I presents the constraints for both parametrizations, along with their interacting counterparts (denoted by the prefix ‘i-’). The CPL and JBP parametrizations are most widely utilized in dynamical DE studies, providing greater flexibility compared to simpler models such as  $w$ CDM, for analysing the evolution of the DE EoS. Moreover, we choose these two particular parametrizations, due to their demonstrated success in alleviating the  $S_8$  tension with SDSS BAO in an interacting setup [20].

To ensure the consistency of our `MontePython` likelihood for DESI DR2 with the `Cobaya` likelihood used by the DESI collaboration, we have first validated the non-interacting cases for the same parametrizations. The constraints obtained for the non-interacting cases (particularly CPL) are found to be fully consistent with those reported by the DESI collaboration [19, 51], confirming the reliability of our pipeline for further exploration of the interacting sectors using `CLASS + MontePython`. We present the full contour plots in Fig. 3, which were generated using `GetDist`<sup>2</sup> [52]. We make the following observations:

### 1. Consistency between SDSS and DESI DR2:

Comparing Table I with Table III of [20], we observe

minor shifts in  $H_0$ ,  $\Omega_{m0}$ ,  $\sigma_{8,0}$ , and  $S_8$ . However, these shifts are statistically insignificant, with all constraints remaining consistent to within  $1\sigma$  between the SDSS and DESI DR2 cases, along with a slight overall increase in precision. Furthermore, a comparison between Fig. 3 and Fig. 5 of [20] reveals identical trends and correlations.

- The tensions:** The Hubble tension is neither alleviated nor worsened in the case with DESI compared to SDSS, although a slight increase in the mean value of  $H_0$  is observed (supposedly driven by DESI). The clustering tension is alleviated in a similar manner to that described in [20] for DESI DR2, with slightly lower mean values for  $S_8$  compared to SDSS, while maintaining the same level of precision within the  $1\sigma$  confidence level. The presence of interaction reduces the  $H_0 - \sigma_{8,0}$  correlation, as shown in the left panel of Fig. 1, a trend that remains consistent across both BAO datasets.
- Nature of dark energy:** The constraints on the EoS parameters ( $w_0$  and  $w_a$ ) from SDSS and DESI DR2 are largely consistent for the interacting cases. As shown in Fig. 1, both interacting and non-interacting models favour a deviation from  $w = -1$ . However, in the phantom limit, the i-CPL and i-JBP models prefer a less strong phantom-like evolution at early times. For CPL,  $w_0 = 0.837 \pm 0.056$  and  $w_a = -0.59^{+0.23}_{-0.21}$ , leading to  $w \approx -1.425$  at high redshifts (see [19, 51]). In contrast, i-CPL shifts the  $w_0 > -1.04$  and  $w_a = -0.33 \pm 0.15$ , making the early universe EoS less phantom ( $w \approx -1.347$ ). For JBP,  $w_0 = -0.807 \pm 0.085$  and  $w_a = -1.09 \pm 0.53$ , whereas i-JBP gives  $w_0 > -1.06$ ,  $w_a = -0.33 \pm 0.3$ . This suggests that the iDMDE models suppress extreme phantom evolution in the early universe while still allowing a transition toward  $w \sim -1$  at lower redshifts.

<sup>2</sup> <https://github.com/cmbant/getdist>

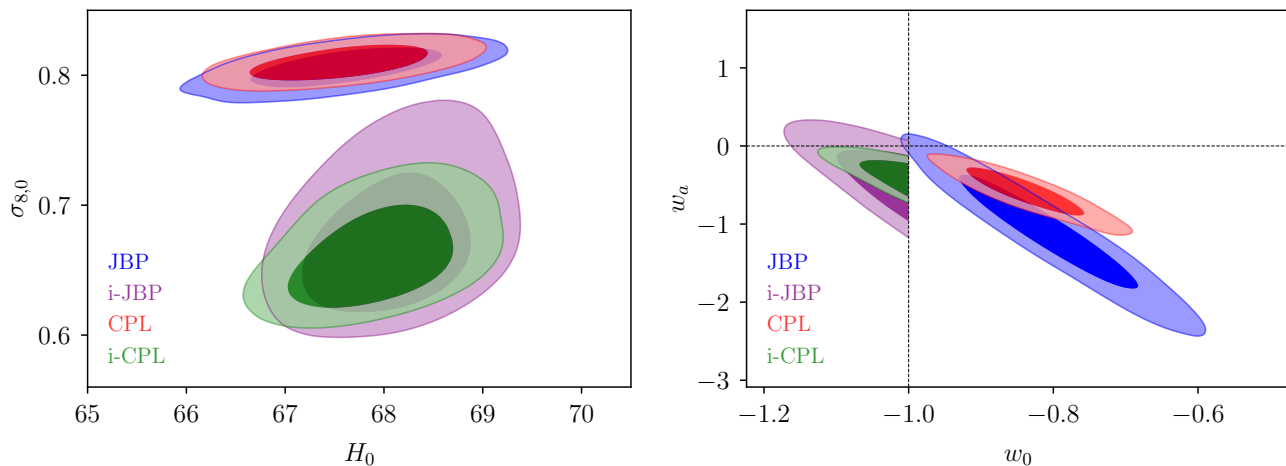


FIG. 1: Constraints on and correlations between  $H_0$  and  $\sigma_{8,0}$ , as well as  $w_0$  and  $w_a$ , are shown for the models considered in this work. The non-interacting cases smoothly incorporate  $w = -1$  crossing using the PPF formalism. In contrast, the interacting cases divide the parameter space into phantom and non-phantom regions - only the phantom case is shown here.

**4. Nature of interaction:** The presence of a positive, non-zero  $Q$  in both interacting models means that dark energy is decaying into dark matter. The interaction helps to gradually suppress deviations from  $w = -1$  at early times compared to non-interacting CPL/JBP models.

When interactions are introduced, different results for  $\sigma_{8,0}$  (and to a lesser extent,  $H_0$ ) emerge in the two regimes. We find that the phantom interacting case helps alleviate the  $S_8$  tension when using the latest DESI DR2 BAO data, with a shift in the mean value towards a lower  $S_8$ , (a direction favoured towards addressing the tension). Appendix A shows that  $S_8$  assumes a higher mean value in the non-phantom case (consistent with our previous findings using SDSS BAO [20]), but it can accommodate lower  $S_8$  values due to reduced precision in the inferred constraint. Thus, despite the preference for a present-day non-phantom EoS in the non-interacting case (with DE perturbations handled using the PPF formalism) across both BAO datasets, the phantom regime appears to yield cosmological parameter estimates, particularly for  $H_0$  and  $S_8$ , that better align with observational constraints when both interactions and dark energy perturbations are considered.

Notably, the surprise comes with the value of  $w_a$ , which largely governs the steep evolution of the EoS with DESI, making it tend to deviate from  $w = -1$  case to a considerable extent at certain redshift regions of its evolution for the non-interacting CPL and JBP models. However, we find that the presence of interactions in the dark sector moderates this steep evolution, making the  $w = -1$  deviation less pronounced compared to the non-interacting cases (see Fig. 2).

At this stage, we interpret this moderation as a combined effect of interactions in the DM-DE sector and

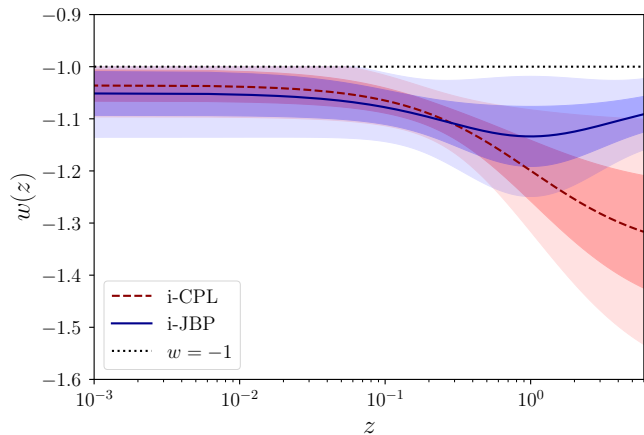


FIG. 2: Plots for the evolution of DE EoS for interacting CPL and JBP models. The best-fit line is shown along with the  $1\sigma$  and  $2\sigma$  confidence intervals in the shaded regions.

dark energy perturbations. Determining which of the two plays a more significant role is a matter for future investigation. However, since the inclusion of perturbations in the non-interacting setup still indicates a deviation from the  $w = -1$  EoS, we anticipate that the primary factor behind reducing the steep evolution is the interaction between the dark sectors.

This leads to an interesting consideration: if DESI's preference for a steeply evolving EoS is indeed significant, it is worth exploring why this preference weakens in the presence of dark sector interactions - a paradigm that remains observationally viable and has shown promise in addressing cosmological tensions.

Indeed, the interaction parameter  $Q$  plays a significant role here, as it is seen that any large deviation from

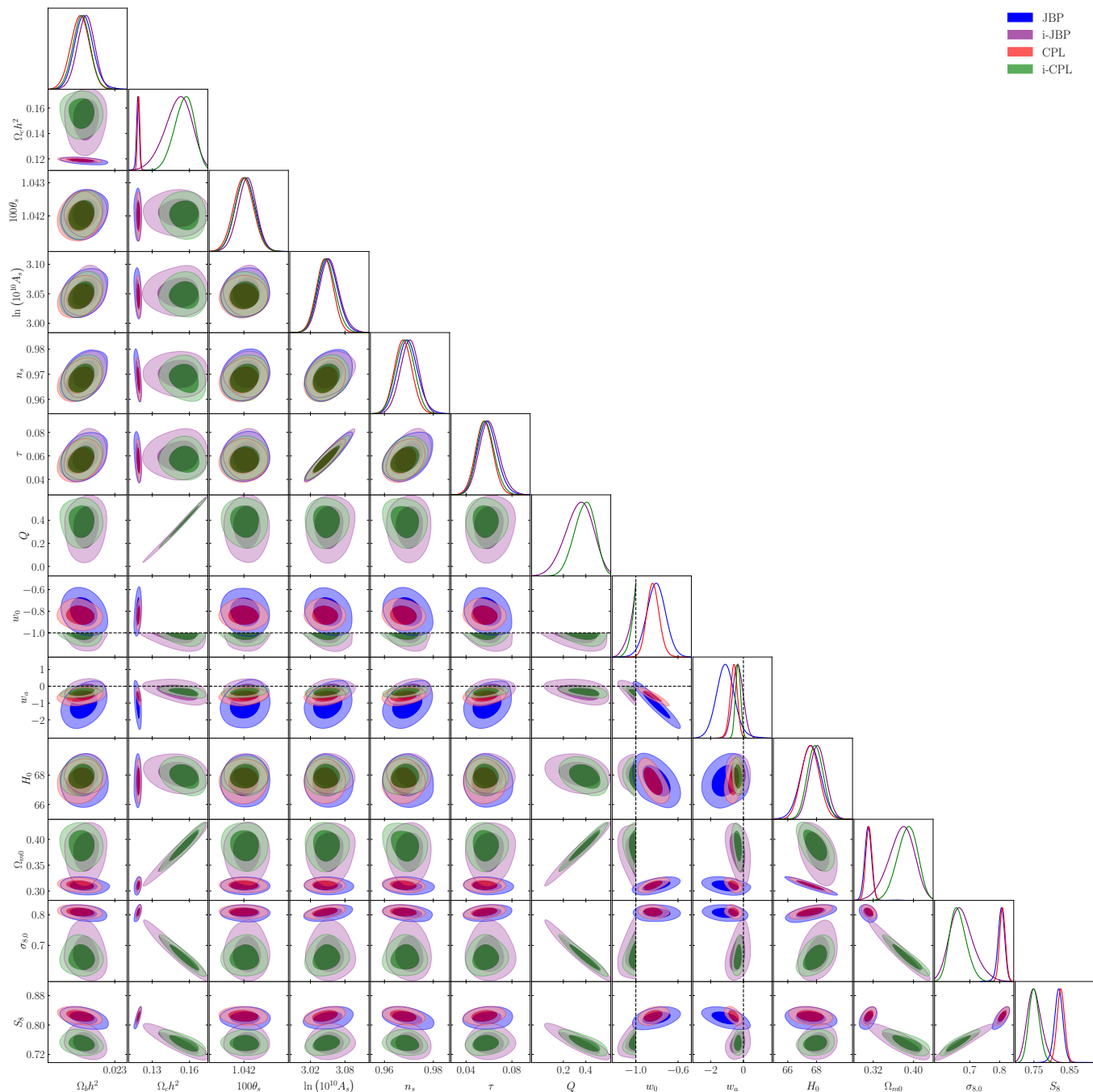


FIG. 3: Comparison of constraints obtained for interacting (phantom regime) and non-interacting models considered in the present work, using combined Planck 2018 + DESI DR2 BAO + Pantheon+ datasets.

$w_a = 0$  in the non-interacting case (as reported by the DESI collaboration) is now being compensated somewhat by the presence of a non-vanishing  $Q$ . Notably, the introduction of the interaction term does not worsen the fit to the data, as indicated by the  $\chi^2$  values in Table I.

Although these conclusions are based on a specific (albeit widely accepted) form of the interaction parameter, it is worthwhile to explore alternative interaction models and examine their impact on cosmological tensions and EoS parameters to draw more general conclusions

about iDMDE sectors using DESI DR2 along with other datasets. Examples of such interactions can be found in [53] and references therein.

In conclusion, in this study we revisited the iDMDE sector scenario in light of the latest DESI DR2 BAO measurements. We found that while DESI's non-interacting dark energy EoS significantly deviates from  $\Lambda$ CDM, the inclusion of interactions in the dark sector moderates this deviation by reducing the preference for a steeply evolving EoS. The interaction plays a key role by reducing

Parameters	i-CPL Non-phantom
$\Omega_b h^2$	$0.02254 \pm 0.00013$
$\Omega_c h^2$	$0.049^{+0.026}_{-0.032}$
$100\theta_s$	$1.04209 \pm 0.00027$
$\ln(10^{10} A_s)$	$3.051 \pm 0.015$
$n_s$	$0.9709 \pm 0.0035$
$\tau$	$0.0595 \pm 0.0077$
$Q$	$-0.52^{+0.17}_{-0.22}$
$w_0$	$-0.764^{+0.093}_{-0.074}$
$w_a$	$-0.184^{+0.090}_{-0.11}$
$H_0$	$67.66 \pm 0.57$
$\Omega_{m0}$	$0.158^{+0.056}_{-0.070}$
$\sigma_{8,0}$	$1.71^{+0.58}_{-0.77}$
$S_8$	$1.14^{+0.20}_{-0.23}$

TABLE II: The mean and  $1\sigma$  constraints obtained for interacting CPL model in the non-phantom regime, using combined Planck 2018 + DESI DR2 BAO + Pantheon+ datasets.

the  $H_0$ - $\sigma_{8,0}$  correlation and easing the clustering tension. Since the phantom regime induces a shift in  $S_8$  towards lower values, thereby helping to address the clustering tension without worsening the Hubble tension, it remains the more interesting case; the non-phantom case on the other hand caused a shift in the other direction with lesser precision in  $S_8$ .

Our results underscore the importance of consistently incorporating perturbations in phantom models, and we suggest that exploring alternative interaction forms could provide further insights into dark sector dynamics, especially in light of novel datasets such as DESI DR2.

*Note:* Although the DES-Y3 [54] and KiDS-Legacy [55] collaborations have recently reported higher values for  $S_8$ , their new methodology awaits further reassessment through a systematic analysis by the community,

considering all potential sources of uncertainty. In this article, we rely on the commonly accepted values of  $S_8$  [45–47, 56].

*The datasets used in this work are publicly available. The modified codes used for this study may be made available upon reasonable request.*

We thank Debarun Paul and Raj Kumar Das for useful discussions. RS acknowledges financial support from ISI Kolkata as a Senior Research Fellow. PM acknowledges financial support from the Anusandhan National Research Foundation (ANRF), Govt. of India under the National Post-Doctoral Fellowship (N-PDF File no. PDF/2023/001986). SP thanks the ANRF, Govt. of India for partial support through Project No. CRG/2023/003984. We acknowledge the use of the Pegasus cluster of the high performance computing (HPC) facility at IUCAA, Pune, India.

### Appendix A: Non-Phantom Interacting Case

Here we show the constraints in the non-phantom regime for the interacting and non-interacting CPL cases for representative purposes. The full contour plots are in Fig. 4 and the constraints are in Table II. We note that there is a peak in the posterior of  $w_0$ , unlike the phantom case. There is also a negative correlation between  $w_a$  and  $Q$ , indicating that deviations in  $w_a$  from 0 can be compensated by negative values of  $Q$ . This behaviour arises as a consequence of restricting our analysis to the non-phantom region, whereas the non-interacting CPL parametrization exhibits an early-phantom-like trend. However,  $S_8$  takes a large value ( $S_8 = 1.14^{+0.20}_{-0.23}$ ) with an order of magnitude worse precision than in the corresponding phantom case. Although this reduces the Gaussian tension on account of larger error bars, the direction of shift in the mean value of  $S_8$  raises doubts on the admissibility of this scenario as a coherent resolution to cosmological tensions.

- 
- [1] A. G. Adame et al. (DESI), *JCAP* **02**, 021, [arXiv:2404.03002 \[astro-ph.CO\]](#).
  - [2] W. Giarè, M. Najafi, S. Pan, E. Di Valentino, and J. T. Firouzjaee, *JCAP* **10**, 035, [arXiv:2407.16689 \[astro-ph.CO\]](#).
  - [3] B. R. Dinda and R. Maartens, *JCAP* **01**, 120, [arXiv:2407.17252 \[astro-ph.CO\]](#).
  - [4] S. Pourojaghi, M. Malekjani, and Z. Davari, *Mon. Not. Roy. Astron. Soc.* **537**, 436 (2025), [arXiv:2408.10704 \[astro-ph.CO\]](#).
  - [5] E. O. Colgáin and M. M. Sheikh-Jabbari, [arXiv \(2024\), arXiv:2412.12905 \[astro-ph.CO\]](#).
  - [6] P. Bansal and D. Huterer, [arXiv \(2025\), arXiv:2502.07185 \[astro-ph.CO\]](#).
  - [7] A. Sousa-Neto, C. Bengaly, J. E. González, and J. Alcaniz, [arXiv \(2025\), arXiv:2502.10506 \[astro-ph.CO\]](#).
  - [8] O. Luongo and M. Muccino, *Astron. Astrophys.* **690**, A40 (2024), [arXiv:2404.07070 \[astro-ph.CO\]](#).
  - [9] M. Cortès and A. R. Liddle, *JCAP* **12**, 007, [arXiv:2404.08056 \[astro-ph.CO\]](#).
  - [10] E. O. Colgáin, M. G. Dainotti, S. Capozziello, S. Pourojaghi, M. M. Sheikh-Jabbari, and D. Stojkovic, [arXiv \(2024\), arXiv:2404.08633 \[astro-ph.CO\]](#).
  - [11] C.-G. Park, J. de Cruz Pérez, and B. Ratra, *Phys. Rev. D* **110**, 123533 (2024), [arXiv:2405.00502 \[astro-ph.CO\]](#).
  - [12] R. Calderon et al. (DESI), *JCAP* **10**, 048, [arXiv:2405.04216 \[astro-ph.CO\]](#).

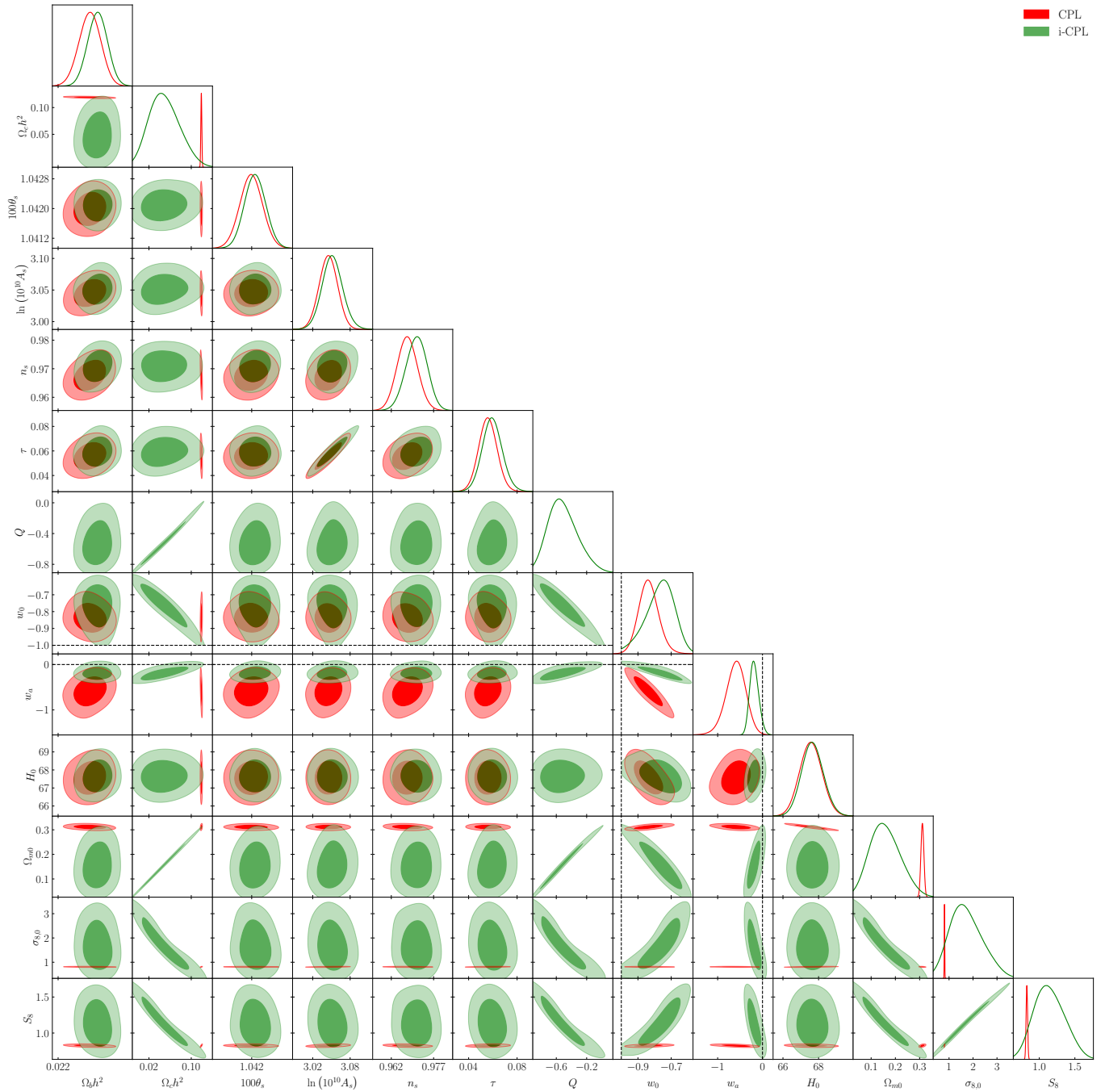


FIG. 4: Comparison of constraints obtained for interacting (non-phantom regime) and non-interacting CPL models considered in the present work, using combined Planck 2018 + DESI DR2 BAO + Pantheon+ datasets.

- [13] K. Lodha et al. (DESI), *Phys. Rev. D* **111**, 023532 (2025), [arXiv:2405.13588 \[astro-ph.CO\]](#).
- [14] N. Roy, arXiv (2024), [arXiv:2406.00634 \[astro-ph.CO\]](#).
- [15] I. D. Gialamas, G. Hütsi, K. Kannike, A. Racioppi, M. Raidal, M. Vasar, and H. Veermäe, *Phys. Rev. D* **111**, 043540 (2025), [arXiv:2406.07533 \[astro-ph.CO\]](#).
- [16] A. Notari, M. Redi, and A. Tesi, *JCAP* **11**, 025, [arXiv:2406.08459 \[astro-ph.CO\]](#).
- [17] P. Mukherjee and A. A. Sen, *Phys. Rev. D* **110**, 123502 (2024), [arXiv:2405.19178 \[astro-ph.CO\]](#).
- [18] P. Mukherjee and A. A. Sen, arXiv (2025), [arXiv:2503.02880 \[astro-ph.CO\]](#).
- [19] M. Abdul Karim et al. (DESI), arXiv (2025), [arXiv:2503.14738 \[astro-ph.CO\]](#).
- [20] R. Shah, P. Mukherjee, and S. Pal, *Mon. Not. Roy. Astron. Soc.* **536**, 2404 (2024), [arXiv:2404.06396 \[astro-ph.CO\]](#).
- [21] E. Di Valentino, O. Mena, S. Pan, L. Visinelli, W. Yang, A. Melchiorri, D. F. Mota, A. G. Riess, and J. Silk, *Class. Quant. Grav.* **38**, 153001 (2021), [arXiv:2103.01183 \[astro-ph.CO\]](#).

- [22] E. Di Valentino *et al.*, *Astropart. Phys.* **131**, 102604 (2021), [arXiv:2008.11285 \[astro-ph.CO\]](#).
- [23] E. Abdalla *et al.*, *JHEAp* **34**, 49 (2022), [arXiv:2203.06142 \[astro-ph.CO\]](#).
- [24] S. Pan and W. Yang, [arXiv:2310.07260](#) [10.1007/978-981-99-0177-7\\_29](#) (2023), [arXiv:2310.07260 \[astro-ph.CO\]](#).
- [25] T.-N. Li, P.-J. Wu, G.-H. Du, S.-J. Jin, H.-L. Li, J.-F. Zhang, and X. Zhang, *Astrophys. J.* **976**, 1 (2024), [arXiv:2407.14934 \[astro-ph.CO\]](#).
- [26] W. Giarè, Y. Zhai, S. Pan, E. Di Valentino, R. C. Nunes, and C. van de Bruck, *Phys. Rev. D* **110**, 063527 (2024), [arXiv:2404.02110 \[astro-ph.CO\]](#).
- [27] W. Giarè, M. A. Sabogal, R. C. Nunes, and E. Di Valentino, *Phys. Rev. Lett.* **133**, 251003 (2024), [arXiv:2404.15232 \[astro-ph.CO\]](#).
- [28] Y. Zhai, M. de Cesare, C. van de Bruck, E. Di Valentino, and E. Wilson-Ewing, [arXiv \(2025\)](#), [arXiv:2503.15659 \[astro-ph.CO\]](#).
- [29] A. Bhattacharyya, U. Alam, K. L. Pandey, S. Das, and S. Pal, *Astrophys. J.* **876**, 143 (2019), [arXiv:1805.04716 \[astro-ph.CO\]](#).
- [30] S. Sinha, *Phys. Rev. D* **103**, 123547 (2021), [arXiv:2101.08959 \[astro-ph.CO\]](#).
- [31] N. Aghanim *et al.* (Planck), *Astron. Astrophys.* **641**, A5 (2020), [arXiv:1907.12875 \[astro-ph.CO\]](#).
- [32] N. Aghanim *et al.* (Planck), *Astron. Astrophys.* **641**, A6 (2020), [Erratum: *Astron. Astrophys.* 652, C4 (2021)], [arXiv:1807.06209 \[astro-ph.CO\]](#).
- [33] N. Aghanim *et al.* (Planck), *Astron. Astrophys.* **641**, A8 (2020), [arXiv:1807.06210 \[astro-ph.CO\]](#).
- [34] D. Scolnic *et al.*, *Astrophys. J.* **938**, 113 (2022), [arXiv:2112.03863 \[astro-ph.CO\]](#).
- [35] J. Lesgourgues, [arXiv \(2011\)](#), [https://github.com/lesgourg/class\\_public](https://github.com/lesgourg/class_public), [arXiv:1104.2932 \[astro-ph.IM\]](#).
- [36] D. Blas, J. Lesgourgues, and T. Tram, *JCAP* **07**, 034, [https://github.com/lesgourg/class\\_public](https://github.com/lesgourg/class_public), [arXiv:1104.2933 \[astro-ph.CO\]](#).
- [37] G. A. Hoerning, R. G. Landim, L. O. Ponte, R. P. Rolim, F. B. Abdalla, and E. Abdalla, [arXiv:2308.05807](#) [10.48550/arXiv.2308.05807](#) (2023), [arXiv:2308.05807 \[astro-ph.CO\]](#).
- [38] M. Lucca and D. C. Hooper, *Phys. Rev. D* **102**, 123502 (2020), [arXiv:2002.06127 \[astro-ph.CO\]](#).
- [39] T. Brinckmann and J. Lesgourgues, *Phys. Dark Univ.* **24**, 100260 (2019), [https://github.com/brinckmann/montepython\\_public](https://github.com/brinckmann/montepython_public), [arXiv:1804.07261 \[astro-ph.CO\]](#).
- [40] B. Audren, J. Lesgourgues, K. Benabed, and S. Prunet, *JCAP* **02**, 001, [https://github.com/brinckmann/montepython\\_public](https://github.com/brinckmann/montepython_public), [arXiv:1210.7183 \[astro-ph.CO\]](#).
- [41] J. Torrado and A. Lewis, *JCAP* **05**, 057, [arXiv:2005.05290 \[astro-ph.IM\]](#).
- [42] M. B. Gavela, D. Hernandez, L. Lopez Honorez, O. Mena, and S. Rigolin, *JCAP* **07**, 034, [Erratum: *JCAP* 05, E01 (2010)], [arXiv:0901.1611 \[astro-ph.CO\]](#).
- [43] M. B. Gavela, L. Lopez Honorez, O. Mena, and S. Rigolin, *JCAP* **11**, 044, [arXiv:1005.0295 \[astro-ph.CO\]](#).
- [44] W. Fang, W. Hu, and A. Lewis, *Phys. Rev. D* **78**, 087303 (2008), [arXiv:0808.3125 \[astro-ph\]](#).
- [45] S.-S. Li *et al.*, *Astron. Astrophys.* **679**, A133 (2023), [arXiv:2306.11124 \[astro-ph.CO\]](#).
- [46] T. M. C. Abbott *et al.* (DES), *Phys. Rev. D* **105**, 023520 (2022), [arXiv:2105.13549 \[astro-ph.CO\]](#).
- [47] T. M. C. Abbott *et al.* (Kilo-Degree Survey, DES), *Open J. Astrophys.* **6**, 2305.17173 (2023), [arXiv:2305.17173 \[astro-ph.CO\]](#).
- [48] M. Chevallier and D. Polarski, *Int. J. Mod. Phys. D* **10**, 213 (2001), [arXiv:gr-qc/0009008](#).
- [49] E. V. Linder, *Phys. Rev. Lett.* **90**, 091301 (2003), [arXiv:astro-ph/0208512 \[astro-ph\]](#).
- [50] H. K. Jassal, J. S. Bagla, and T. Padmanabhan, *Phys. Rev. D* **72**, 103503 (2005), [arXiv:astro-ph/0506748](#).
- [51] K. Lodha *et al.*, [arXiv \(2025\)](#), [arXiv:2503.14743 \[astro-ph.CO\]](#).
- [52] A. Lewis, [arXiv \(2019\)](#), <https://github.com/cmbant/getdist>, [arXiv:1910.13970 \[astro-ph.IM\]](#).
- [53] B. Wang, E. Abdalla, F. Atrio-Barandela, and D. Pavón, *Rept. Prog. Phys.* **87**, 036901 (2024), [arXiv:2402.00819 \[astro-ph.CO\]](#).
- [54] T. M. C. Abbott *et al.* (DES), [arXiv \(2025\)](#), [arXiv:2503.13632 \[astro-ph.CO\]](#).
- [55] A. H. Wright *et al.*, [arXiv \(2025\)](#), [arXiv:2503.19441 \[astro-ph.CO\]](#).
- [56] T. Hamana *et al.*, *Publ. Astron. Soc. Jap.* **72**, 16 (2020), [Erratum: *Publ. Astron. Soc. Jap.* 74, 488-491 (2022)], [arXiv:1906.06041 \[astro-ph.CO\]](#).